RSC Advances

ROYAL SOCIETY OF CHEMISTRY

www.rsc.org/advances

RSC Advances

PAPER

A novel high-energetic and good-sensitive cocrystal composed of CL-20 and TATB by a rapid solvent/non-solvent method

Received 00th January 20xx,
Accepted 00th January 20xx

DOI: 10.1039/x0xx00000x

www.rsc.org/

Haifeng Xu,[ab] Xiaohui Duan,*[a] Hongzhen Li,*[b] and Chonghua Pei[a]

Due to insolubility of TATB in majority of organic solvents, it is very difficult to prepare the cocystals of TATB. In this work, through a rapid nucleation solvent/non-solvent process, a novel cocrystal explosive, CL-20 (2,4,6,8,10,12-hexanitro-2,4,6,8,10,12-hexaazaisowurtzitane)/TATB (1,3,5-Triamino-2,4,6-trinitrobenzene), has been successful prepared. The cocrystal is characterized by scanning electron microscopy (SEM), X-ray powder diffraction (XRD), Fourier Transform Infrared spectroscope (FT-IR) spectra, Raman spectra, thermogravimetric/differential scanning calorimetric (TG-DSC), and High performance liquid chromatography (HPLC). The SEM results indicate that the cocrystal particles are homogeneous with the average particle size of about 3-5 μm, and the morphology of cocrystal is completely different from primary materials. XRD and Raman analyses confirm that the cocrystal has unique peak patterns with large difference from CL-20 and TATB. IR and Raman spectra suggest that there exist hydrogen-bonding interactions between CL-20 and TATB molecules. The density determination, the weight loss on one step and the only exothermic peak in thermal analysis curves further illustrate that CL-20/TATB cocrystal is a new substance instead of individual crystallization of CL-20 and TATB. In CL-20/TATB cocrystal, the molar ratio of CL-20 and TATB is 3:1 determined by HPLC. Thermal analysis and detonation parameters calculation shows that the cocrystal has excellent thermal stability and high energy-release efficiency. Impact sensitivity test indicates that the sensitivity of cocrystal is sufficiently reduced relative to CL-20. For CL-20/TATB cocrystal, its detonation performance is superior to HMX and impact sensitivity is almost the same with HMX.

1. Introduction

Energetic materials (EMs) i.e. explosives, propellants, and pyrotechnics, play an important role in both civilian and military applications.[1, 2] As a representative of a category compounds with plenty of stored chemical energy in the molecular structures, EMs exist an inherent safety−power contradiction.[3] Thus, higher performance such as good thermal stability, higher power and detonation velocity, higher density, or enhancement of insensitivity has always been a prime requirement in the field of energetic materials. In order to tailor and improve EMs properties, most of the researchers use some traditional strategies include synthesizing new energetic compounds,[4, 5] improving the quality of high explosive crystals,[6, 7] preparing nanoscaling particles of explosives[8-12] and adding insensitive compounds or coating by physics skill.[13-17] Although these methods have made some achievements, there still exist some problems. For example, synthesis of new materials is still unable to acquire an ideal simple substance explosive.[4] Also, the fundamental problem of the sensitivity of explosives can't be solved by recrystallization to improve the quality of explosive crystals.[18] In addition, nanocrystallization of explosives particles are confronted with serious agglomeration, though it can strongly change the sensitivity and performance of EMs. Plastic bonded explosives (PBXs) have been widely researched in EMs fields. Nevertheless, it requires lots of inert additives resulting in the energy reduction.[19]

In recent years, an alternative way to improve the properties of explosives is cocrystallizing, which is widely used for the pharmaceutical chemical,[20, 21] attracts the interest of numerous related scientists and engineers.[22-35] Cocrystallization, consisting of two or more components in a defined ratio via non-covalent interactions include hydrogen bonds, π-stacking, or van der Waals forces interaction,[36, 37] is completely different from the traditional methods. It is emerging as an attractive approach to improve some key properties including density, thermal stability, oxygen balance, sensitivity, and detonation performance of energetic materials. Thus, cocrystallization engineering is an effective way to modify the integrated performance of CL-20,[38, 39] a novel caged nitramine explosive with the highest energy density, good oxygen balance and high explosive power. According to actual measurement, many aspects of its performance, such as oxygen balance, detonation velocity and density, are all superior to the current military standard explosive HMX and its detonation energy release was found to be approximately 14% higher than that of HMX.[40] Its high detonation velocity and detonation pressure make CL-20 a suitable candidate for a wide range of military and commercial purpose. Unfortunately, its high mechanical sensitivity limits further application,[41, 42] and it is relatively easily detonated by physical forces in comparison to other secondary explosives.[40] Hence, insensitivity of CL-20 is becoming increasingly important. Cocrystallizing with insensitive explosive is indeed a hopeful strategy to decrease its sensitivity. According to

[a]State Key Laboratory Cultivation Base for Nonmetal Composites and Functional Materials, Southwest University of Science and Technology, Mianyang 621010, P. R. China
[b]Institute of Chemical Materials, China Academy of Engineering Physics, Mianyang 621900,Sichuan, P. R. China

the literature, some CL-20 cocrystal explosives have been prepared to improve its sensitivity.[2, 24-27] For example, Bolton and co-workers have successfully obtained the CL-20/TNT cocrystal.[24] This cocrystal reduces the mechanical impact sensitivity relative to pure CL-20, but it also largely decreased explosive power due to the incorporation of TNT. And then CL-20/HMX cocrystal was reported by them.[25] Although this cocrystal exhibit greater power, its sensitivity has not improved obviously. CL-20/BTF cocrystal is also not an ideal cocrystal explosive because of its poor detonation properties.[26]

As we all know, TATB, the so-called wood explosive, is widely used in military and civilian application because of its moderate power, thermal stable, and insensitivity.[43, 44] It is more insensitive than TNT, and its energy density is higher than TNT. Density of TATB is 1.938 g/cm^3, much higher than TNT, 1.654 g/cm^3.[45] Pure TATB is an inert explosive towards heat, light, friction, and mechanical impact, which can attribute to its graphite-like layered structure. This layered structure of TATB with strong inter-molecular and intra-molecular hydrogen bonds, makes it difficult to form hot spots as external stir energy can be easily transferred to the slide between neighboring layers.[46, 47] So, we expect that the TATB/CL-20 cocrystal will have better comprehensive performance, such as higher energy and lower sensitivity. In our previous work, the cocrystal of HMX and TATB had been prepared through a slowly solvent/non-solvent method. Since the molar ratio of HMX:TATB is 8:1, it may be more reasonable to name it as a kind of doped cocrystal.[23] Besides, the cocrystals of TATB have not been reported, and the possible reason can be attributed to the insolubility of TATB in most organic solvents.[48] In this work, we selected and prepared specific solvents to increase the solubility of TATB and made the CL-20 and TATB precipitate at the same time to prepare CL-20/TATB cocrystal through a rapid nucleation solvent/non-solvent (S/NS) process. Compared to conventional method for the preparation of cocrystal explosive, slow evaporation solvents, this method has obvious advantage in facile high-yielding production. The structure and performance of CL-20/TATB cocrystal have been characterized by various methods. The effective characterization results give us sufficient confidence in the successful preparation of CL-20/TATB cocrystal though lacking of the crystallography data of single crystal.

2. Experimental

2.1 Materials

Raw CL-20 (ε polymorph) and TATB (Fig. 1), provided by Institute of Chemical Materials Chinese Academy of Engineering Physics (CAEP), are white and fluorescence green crystalline powder, respectively. DMSO purchased from the Chengdu Ke Long Chemical Reagent Factory and ultrapure water acted as solvent and nonsolvent, respectively.

2.2 Preparation of CL-20/TATB Cocrystal

The cocrystal explosive was prepared by solvent/non-solvent (S/NS) method, a rapid nucleation process. Firstly, two specific solutions of CL-20 and TATB were prepared at 25℃, respectively.

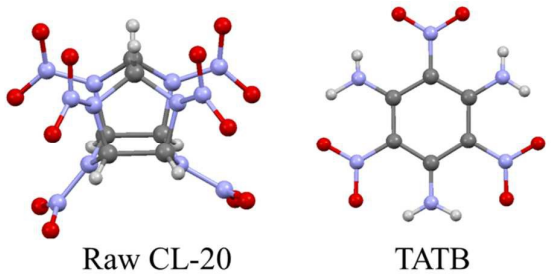

Fig. 1 Chemical structures of raw CL-20, $C_6H_6N_{12}O_{12}$ and TATB, $C_6H_6N_6O_6$

And, the two solutions were rapidly poured into the ultrapure water at the same time. After that, the mixed solution was stirred 1.5 hours and then standing for overnight. Then, the mixed solution was filtrated and the product was washed 3-5 times with ultrapure water to remove the solvent. At last, the sample was freeze-dried and the production rate was 75.5%.

2.3 Characterizations

Scanning electron microscopy (SEM) was conducted on a ULTRA 55 (ZEISS, Germany) field emission scanning electron microscope operating at an accelerating voltage of 5 kV, equipped with an energy dispersive X-ray spectroscopy (EDS). The power X-ray diffraction (XRD) patterns were recorded with a PANalytical X'Pert PRO instrument (Cu Kα, λ= 0.15406 nm, 45 kV, 50 mA, Rigaku D/max-RB, Netherlands). Images were integrated from 3° to 80° with a 0.05° step size using AreaMax 2 software. Raman spectra were measured with inVia Raman spectrometer using a Ar laser (λ=514.5 nm) and a semiconductor laser (λ=785 nm). The maximum output power is 1.7 mW of the light spot of the inVia Raman spectrometer and the spectra resolution is 1 cm^{-1}. Fourier Transform Infrared spectroscope (FT-IR) spectra were measured at 0.4 cm^{-1} resolution on Spectrum One (PE, USA) spectrometer and the IR data were collected in the range of 400–4000 cm^{-1}. High performance liquid chromatography (HPLC) analysis was conducted on an Agilent 1260 HPLC system using a 20 RBAX SB-C18 analytical column (150 × 4.6 mm ID) at 30 ℃ column temperature.

2.4 Performance Test

2.4.1 Thermal Analysis

Simultaneous differential scanning calorimetry (DSC) and thermogravimetry (TG), namely simultaneous DSC-TG curves were conducted with United States SDT Q600 synchronous thermal analyzers at a heating rate of 10 ℃·min^{-1} in N_2 atmosphere over the range 20–500 ℃ with Al_2O_3 as reference. Sample (0.5-2 mg weighed to a precision of 0.0001 mg) was weighed into crimped aluminum pans, pierced to allow vapor to escape, and pressed to increase contact between the pan and sample.

2.4.2 Impact sensitivity

The impact sensitivity testing of the cocrystal was determined using an in-house-constructed drop-weight test with a BAM impact sensitivity instrument according to international standard method. The bump head of BAM impact sensitivity instrument is made of

chilled steel (Rockwell hardness is 60-63), minimum diameter is 25 mm, impact loading include 0.5 kg, 1 kg, 2 kg, 5 kg, 10 kg. Impact energy range is 0.5 J-10 J. Drop high range in 0-1000 mm, atmosphere temperature of 25 ℃, and humidity of 85% RH. And sample measured with 30 mm^3 of cylinder volume.

2.4.3 Density and Detonation Properties

The density was test by Crystal Density Gradient Instrument of Institute of Chemical Materials, China Academy of Engineering Physics. The detonation properties including detonation velocity and detonation pressure at theoretical maximum density (TMD) were calculated by the linear output thermodynamic user-friendly software code.

3. Results and Discussion

3.1. Characterizations

3.1.1 Morphology

Crystal quality such as crystal size, crystal shape, crystal surface, and crystal defects play an important role during safer storage, transport, and handling of munitions items and explosives while maintaining their performance. These physicochemical parameters may also affect the detonation initiation spots of the explosive.[49] The crystal morphologies of the cocrystal and the raw materials are shown in Fig. 2. In Fig. 2, we can see that the morphology of cocrystal is obviously different from those of raw materials. Raw CL-20 crystals are colorless cambiform with integrated crystal surface (Fig. 2a), and TATB raw material is irregularity bulk crystals (Fig. 2b), whereas the CL-20/TATB cocrystal exhibits colorless tetrahedron morphology with smooth and integrated surface (Fig. 2c, d and e). The top left inset e of photograph d shows a magnified image of the area outlined in red. The SEM images show unambiguously that particle size of the cocrystal is uniform and the average particle size is about 3-5 μm.

3.1.2 X-ray Diffraction

The CL-20/TATB cocrystal structure can be distinguished from CL-20 and TATB via powder X-ray diffraction (PXRD). Fig. 3 shows the PXRD patterns including cocrystal, raw CL-20 and TATB, and different polymorphs of CL-20. From the Fig. 3, we can find that the main diffraction angles of CL-20/TATB cocrystal respectively localized at 30.18°, 27.86°, 22.57°, 14.89° are evidently different from the raw materials TATB and CL-20 with different polymorphs. In the 2ϑ range of 10–40°, some peaks of CL-20 and TATB disappear, such as 10.75°, 12.61°, 25.79° of CL-20 and 20.75°, 23.84°, 42.26° of TATB, and new peaks localized at 15.00° and 39.86° are observed in the diffraction pattern of the cocrystal. These differences enable easy distinguishing between the cocrystal and pure TATB or various polymorphs of CL-20 as show in Fig. 3. The unique XRD patterns of cocrystal indicate that it is a new substance instead of the separate crystallization of raw materials. Considering the rich polymorphism of CL-20, we compared XRD peaks of the cocrystal with each kind of crystal type of CL-20. And the results indicate that the peaks of cocrystal were different from all of types of CL-20.

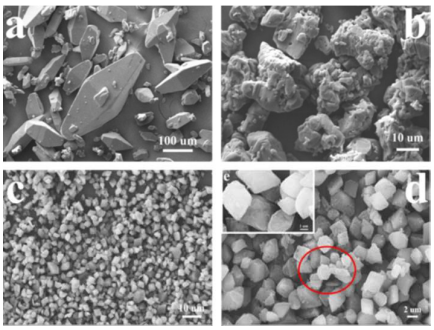

Fig. 2 SEM micrographs of the raw CL-20, TATB and CL-20/TATB cocrystal: (a) raw CL-20, (b) TATB, (c) CL-20/TATB cocrystal and (d), (e) high magnification of CL-20/TATB cocrystal

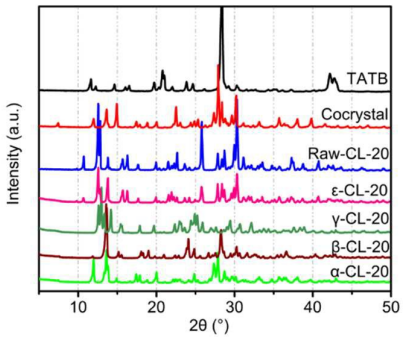

Fig. 3 XRD spectra of α-CL-20, β-CL-20, γ-CL-20, ε-CL-20, raw CL-20, TATB and CL-20/TATB cocrystal

3.1.3 Raman Spectroscopy

Raman spectroscopic is another useful means for characterization of cocrystals, which show the vibrational modes of the cocrystal are different from those of the starting materials.[50-53] Full understanding of the effects of cocrystal formation on the vibrational modes of motion is obtained by the complete assignment of the spectra of the starting materials and of the cocrystal. The Raman spectra of raw CL-20, TATB, and cocrystal are given in Fig. 4. A comparison of the spectra reveals that there are several band shifts occurring between the individual components and the cocrystal. As shown in Fig. 4, in the cocrystal, the band at 126.6 cm^{-1} (NO_2 deformation) of CL-20 shifts to lower wavenumber at 112.1 cm^{-1}, and the bands at 317.9 and 344.9 cm^{-1} (NO_2 twisting vibration and cage skeleton vibration) of CL-20 shift to 309.7 and 336.7 cm^{-1}, respectively. Moreover, the bands at 3032 and 3048 cm^{-1} (C-H stretching) of CL-20 shift higher wavenumbers at 3038 and 3055 cm^{-1}, the band at 1165 cm^{-1} (C-N stretching in C-NH_2) of TATB shifts to 1169 cm^{-1} and the band at 3222 cm^{-1} (NH_2 stretching) of TATB shifts to 3228 cm^{-1} shown in the top right inset b of Fig. 4. At the same time, the bands at 192.3 and 264.7 cm^{-1} (cage deformation) of CL-20 and the band at 3322 cm^{-1} of TATB disappear in the cocrystal, and a strong band at 281.2 cm^{-1} has been observed. On the other hand, the Raman peaks of cocrystal at 386.0 and 881.8 cm^{-1} ring deformation have become more stronger compared with TATB. In addition, following literature report,[54] the Raman spectrum

of this cocrystal is completely different from four polymorphs of CL-20 learning from the top left inset a of Fig. 4. All these changes may be mainly attributed to the hydrogen bonds interactions between $–NO_2$ of CL-20 and $–NH_2$ of TATB.

3.1.4 FT-IR and HPLC

To determine whether impurities exist in the cocrystal and the interactions between CL-20 and TATB molecules, FT-IR spectra of raw CL-20, TATB and CL-20/TATB cocrystal have be measured. As a whole, the absorptions of the cocrystal (Fig. 5a) are similar to those of raw materials, but they still have differences more or less. For the CL-20/TATB cocrystal (Fig. 5a), some absorptions on 979.3, 942.9, 883.4, 722.9, 659.0 and 566.3 cm^{-1} representing mixing vibrations of CL-20 are shifted to 989.9, 951.4, 879.7, 717.5, 657.2 and 563.7 cm^{-1} respectively, and the peak strength has changed. Meanwhile, 1223.3, 1175.2, 699.3, and 446.3 cm^{-1} of mixing vibrations of TATB are weakened and shifted to 1228.3, 1174.9, 717.5 and 447.5 cm^{-1}. As to CL-20/TATB cocrystal, relative to the raw materials, the absorptions on 444.5, 566.3, 979.3 (mixing vibration of CL-20), 854.6 (C-C stretching of CL-20), and 1588.8 cm^{-1} (N=O stretching of CL-20) are weakened or diminished. And according to previously report (see Fig. 5b),[55] a triplet-like feature near 850 cm^{-1} (751, 835, and 880 cm^{-1}) and the low intensity absorption on 3695 cm^{-1} that is shifting from α-CL-20 sharp hydrate peak (3700 cm^{-1}), we infer that the molecular conformation of CL-20 in CL-20/TATB cocrystal is the same as that in α-CL-20 polymorph. According to the above analysis, we can infer that there may exist hydrogen bonds interactions between CL-20 ($–NO_2$) and TATB ($–NH_2$) molecules. In addition, quantitative results from the HPLC determinations confirm that the mass percents of CL-20 and TATB in the CL-20/TATB cocrystal are 83.5% and 16.5%, respectively, corresponding to molar ratio 3:1.

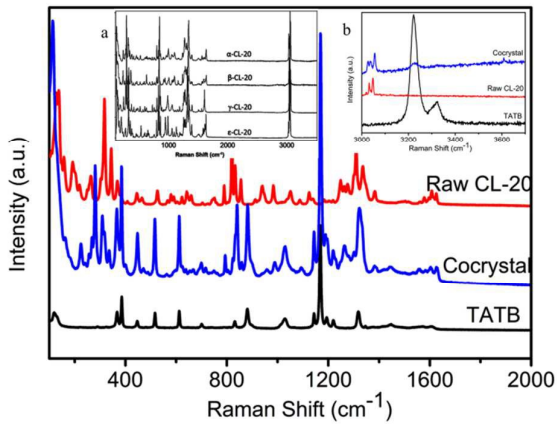

Fig. 4 Raman spectra of raw CL-20, TATB, and CL-20/TATB cocrystal. Top left inset a is literature data of four polymorphic of CL-20 from ref. 54, and the top right inset b is high wavenumber region

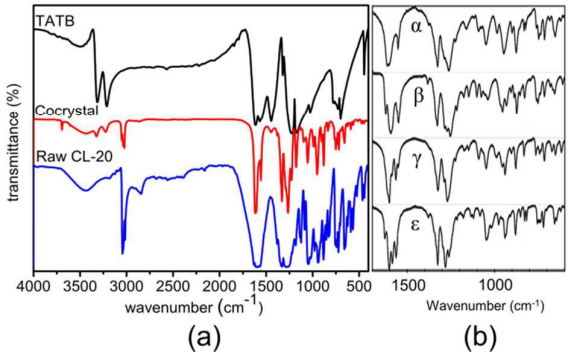

Fig. 5 FT-IR spectra of raw CL-20, TATB and CL-20/TATB cocrystal show in Fig. 5a. Right inset b is literature data of four polymorphic of CL-20 from ref. 55

3.2 Performance Test

3.2.1 Thermal Analysis

The thermal behavior of the cocrystal is examined by simultaneous DSC-TG**.** From the DSC and TG curves in Fig. 6, it is clear that the thermal behaviour of cocrystal is obviously different from its raw materials, and the differences in thermal stability of raw CL-20 and TATB further suggest the formation of a cocrystal. The DSC profile curve reveals a strong exothermic peak at 231.8 ℃ attributed to the decomposing event of the cocrystal, which is distinctly lower than those of the pure CL-20 (245.57 ℃) and TATB (380.89 ℃). The exothermic peak of the cocrystal is in advance compared with CL-20 and TATB, indicating that thermal decomposition activity of cocrystal higher than those of CL-20 and TATB. Besides, a weak endothermic peak at 208.15 ℃ is observed in cocrystal with an increase by approximate 50 ℃ relative to the phase transition temperature ($\varepsilon \rightarrow \gamma$) of CL-20, 161.93 ℃.[56] The temperature at 208.15 ℃ may be considered as the phase transition temperature of cocrystal. In the TG profile of the cocrystal, a constant weight is observed in the temperature range of 0–228.53 ℃, implying no solvent molecule. And then a rapid weight loss on one step appears from 228.53 to 240 ℃, corresponding to a drastic exotherm in the DSC trace of the cocrystal. At the same time, it also illustrates this is our target cocrystal compound instead of mixture, and this is further confirmed by the thermal behavior of the physical mixture of the CL-20 and TATB, which has an obvious two-step weight loss in TG curve.

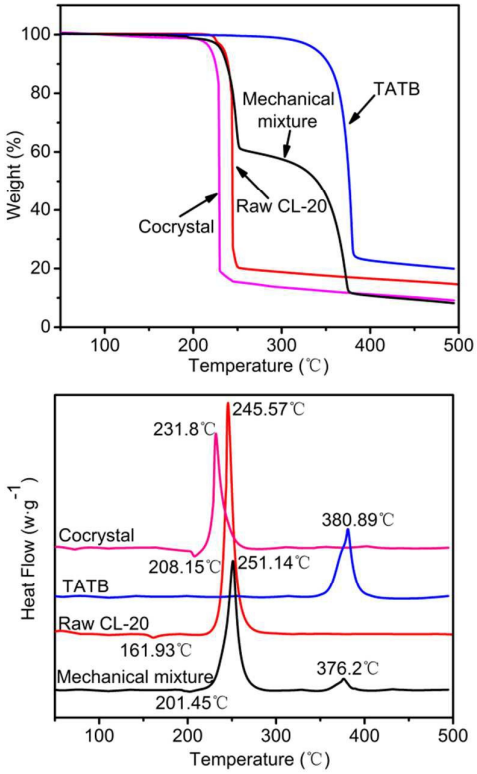

Fig. 6 TG and DSC curves of raw CL-20, TATB and CL-20/TATB cocrystal and mechanical mixture of CL-20 and TATB

3.2.2 Sensitivity Test

In order to evaluate CL-20/TATB cocrystal for potential utilization in the application of explosives, the mechanical sensitivity of the raw CL-20, CL-20/TATB cocrystal, and physical mixture of CL-20 and TATB are investigated by BAM impact sensitivity instrument, a means of an in-house constructed drop-weight test, and 30 mm^3 samples are struck with a drop weight 0.5 kg. With this method, the minimum energy value of detonation of CL-20 is 2.25 J, physical mixture is 2.5 J, and CL-20/TATB cocrystal is 3 J (see Fig. 7). Apparently, the minimum energy value of the CL-20/TATB cocrystal detonation is higher than raw CL-20 and the physical mixture. This result is keeping with most of the cocrystals reported before and further confirms that cocrystallization provides an effective method to ameliorate the sensitivity of explosives. In addition, the cocrystal has similar sensitivity with HMX which has best comprehensive property and is widely used.

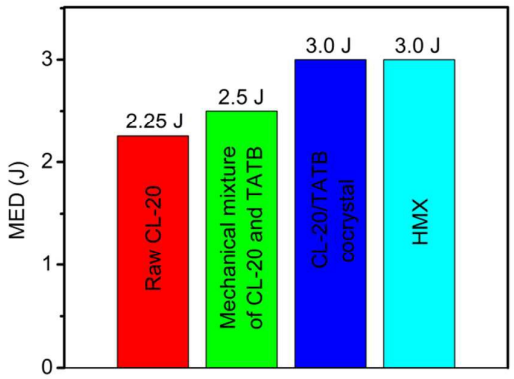

Fig. 7 Results for sensitivity of raw CL-20, mechanical mixture of CL-20 and TATB, and CL-20/TATB cocrystal. MED is Minimum energy value of detonation in Fig.7

3.2.3 Density and Detonation Properties

In terms of energetic materials, there are many important properties of explosive related to the density, including detonation properties, sensitivity and thermal stability, etc. So, searching high density of explosive is beneficial to design and synthesis ideal explosive. Density is one of the characteristics of the materials and the density of each material has its unique. Therefore, we test the density of CL-20/TATB cocrystal, raw CL-20 and TATB at room temperature, and the results are shown in table 1. There is no stratification phenomenon during the testing process of the CL-20/TATB cocrystal and the only density value of 1.960 g/cm^3 means a pure phase. The density of the cocrystal is between two densities of raw materials. To energetic materials, the density is a favorable factors for evaluate their detonation performance. According to the relationship between the detonation property and density of the explosive, we can predict the value of the detonation velocity and detonation pressure about the cocrystal by the linear output thermodynamic user-friendly software code [56-58] as follow:

$$F = 100 \times \frac{nO + nN - \left(\frac{nH}{2nO}\right) + \left(\frac{A}{3}\right) - \left(\frac{nB}{1.75}\right) - \left(\frac{nC}{2.5}\right) - \left(\frac{nD}{4}\right) - \left(\frac{nE}{5}\right)}{MW} - G \quad (1)$$

$$\mathrm{D} = \frac{F - 0.26}{0.55} \quad (2)$$

$$\mathrm{P} = \rho_0 D^2 (1 - 0.713\rho_0^{0.07}) \quad (3)$$

Where *F* is detonation factor, *D* is detonation velocity in km/s, *P* the detonation pressure in GPa. *n*O, *n*N, *n*H are number of oxygen, nitrogen and hydrogen atoms in a molecule. *n*B is number of oxygen atoms in excess of those already available to form CO_2 and H_2O. *n*C is number of oxygen atoms doubly bonded directly to carbon as in carbonyl, *n*D number of oxygen atoms singly bonded directly to carbon, and *n*E number of nitro groups existing either as in a nitrate ester configuration or as a nitric acid salt such as hydrazine mono nitrate. *A* =1 if the compound is aromatic otherwise *A*=0, *G*=0.4 for liquid explosive, and *G*=0 for solid explosive. ρ_0 is the initial density of the unreacted explosive in g cm^3.

The results shown in Table 1 indicate that the detonation velocity and detonation pressure of cocrystal are slightly reduced relative to CL-20, but much higher than those of TATB. The

detonation properties of cocrystal are better than the current military standard explosive HMX due to larger density of 1.960 g/cm^3.

Table1. Detonation properties and densities for raw CL-20, TATB and CL-20/TATB cocrystal

samples	Density (g/cm^3)	Detonation properties	
		Detonation velocity(m/s)	Detonation pressure(GPa)
Raw CL-20	2.038	9382	46.6
TATB	1.913	8036	31.4
CL-20/TATB cocrystal	1.960	9127	41.3
HMX	1.906	9110	39.5

4. Conclusions

A novel energetic cocrystal explosive CL-20/TATB with a 3:1 molar ratio has been successful prepared by applying a rapid nucleation solvent/non-solvent method. Different from the raw materials, CL-20/TATB cocrystal presents colorless tetrahedron with smooth and integrated surface, and the particle size is very uniform with the average particle size of about 3-5 μm. The difference in XRD pattern and Raman spectrum of CL-20/TATB cocrystal from CL-20 and TATB means the formation of a new crystal phase, which is further verified by the density determination and the thermal analysis. The density of CL-20/TATB cocrystal is 1.960 g/cm^3, between CL-20 and TATB. The only exothermic peak at 231.8 ℃ is distinctly lower than those of CL-20 (245.57 ℃) and TATB (380.89 ℃), and the phase transition temperature located at 208.15℃ delays 46.22 ℃ relative to CL-20 (161.93 ℃). Based on the density value, detonation velocity and detonation pressure of CL-20/TATB cocrystal are calculated to be 9127 m/s and 41.3 GPa, respectively, a slight decrease compared to CL-20. These data indicate that CL-20/TATB cocrystal exhibits high energy release efficiency and excellent thermal stability. The mechanical sensitivity of CL-20/TATB cocrystal is decreased from 2.25 J of CL-20 to 3 J. Compared with the current military standard explosive HMX, the detonation properties of CL-20/TATB cocrystal are improved obviously and the sensitivity is almost the same. Besides, rapid nucleation solvent/non-solvent method in this work has prominent advances in high purity of cocrystal, short crystallization time, and easy scaled technology, which provide strong fundament for the practical application of CL-20/TATB cocrystal explosive.

Acknowledgments

We are very grateful for the financial help from the Sichuan Province Key Laboratory for Nonmetal Composites and Functional Materials (No.11zxfk23), the Postgraduate Innovation Fund Project by Southwest University of Science and Technology (No.15ycx006), and Innovation Team Construction Program of Southwest University of Science and Technology (No.14tdfk06).

Notes and references

1. K. B. Landenberger and A. J. Matzger, *Cryst. Growth Des.*, 2012, **12**, 3603-3609.
2. D. I. A. Millar, H. E. Maynard-Casely, D. R. Allan, A. S. Cumming, A. R. Lennie, A. J. Mackay, I. D. H. Oswald, C. C. Tang and C. R. Pulham, *CrystEngComm*, 2012, **14**, 3742.
3. A. K. Sikder and N. Sikder, *J Hazard Mater*, 2004, **112**, 1-15.
4. *US Pat.*, 20040216822 A1, 2004.
5. A. Elbeih, A. Husarova and S. Zeman, *Cent. Eur. J. Energ. Mater.*, 2011, **8**, 173-182.
6. A. E. D. M. van der Heijden, R. H. B. Bouma and A. C. van der Steen, *Propellants, Explos., Pyrotech.*, 2004, **29**, 304-313.
7. H. Kröber and U. Teipel, *Propellants, Explos., Pyrotech.*, 2008, **33**, 33-36.
8. Y. Bayat, M. Zarandi, M. A. Zarei, R. Soleyman and V. Zeynali, *J Mol Liq*, 2014, **193**, 83-86.
9. Y. Bayat and V. Zeynali, *J. Energ. Mater.*, 2011, **29**, 281-291.
10. J. Liu, W. Jiang, Q. Yang, J. Song, G.-z. Hao and F.-s. Li, *Defence Technology*, 2014, **10**, 184-189.
11. X. D. Guo, G. Ouyang, J. Liu, Q. Li, L. X. Wang, Z. M. Gu and F. S. Li, *J. Energ. Mater.*, 2015, **33**, 24-33.
12. G. Yang, F. Nie, H. Huang, L. Zhao and W. Pang, *Propellants, Explos., Pyrotech.*, 2006, **31**, 390-394.
13. B. C. Tappan and T. B. Brill, *Propellants, Explos., Pyrotech.*, 2003, **28**, 223-230.
14. S. S. Samudre, U. R. Nair, G. M. Gore, R. Kumar Sinha, A. Kanti Sikder and S. Nandan Asthana, *Propellants, Explos., Pyrotech.*, 2009, **34**, 145-150.
15. C.-W. An, F.-S. Li, X.-L. Song, Y. Wang and X.-D. Guo, *Propellants, Explos., Pyrotech.*, 2009, **34**, 400-405.
16. A. K. Nandi, M. Ghosh, V. B. Sutar and R. K. Pandey, *Cent. Eur. J. Energ. Mater.*, 2012, **9**, 119-130.
17. Z. Ma, B. Gao, P. Wu, J. Shi, Z. Qiao, Z. Yang, G. Yang, B. Huang and F. Nie, *RSC Adv.*, 2015, **5**, 21042-21049.
18. J. H. Urbelis and J. A. Swift, *Cryst. Growth Des.*, 2014, **14**, 1642-1649.
19. L. Yu, H. Ren, X. Y. Guo, X. B. Jiang and Q. J. Jiao, *J Therm Anal Calorim*, 2014, **117**, 1187-1199.
20. N. Chieng, M. Hubert, D. Saville, T. Rades and J. Aaltonen, *Cryst. Growth Des.*, 2009, **9**, 2377-2386.
21. D. R. Weyna, T. Shattock, P. Vishweshwar and M. J. Zaworotko, *Cryst. Growth Des.*, 2009, **9**, 1106-1123.
22. K. B. Landenberger and A. J. Matzger, *Cryst. Growth Des.*, 2010, **10**, 5341-5347.
23. J. P. Shen, X. H. Duan, Q. P. Luo, Y. Zhou, Q. L. Bao, Y. J. Ma and C. H. Pei, *Cryst. Growth Des.*, 2011, **11**, 1759-1765.
24. O. Bolton and A. J. Matzger, *Angew Chem Int Ed*, 2011, **50**, 8960-8963.
25. O. Bolton, L. R. Simke, P. F. Pagoria and A. J. Matzger, *Cryst. Growth Des.*, 2012, **12**, 4311-4314.
26. Z. Yang, H. Li, X. Zhou, C. Zhang, H. Huang, J. Li and F.

Nie, *Cryst. Growth Des.*, 2012, **12**, 5155-5158.
27. C. Y. Guo, H. B. Zhang, X. C. Wang, J. J. Xu, Y. Liu, X. F. Liu, H. Huang and J. Sun, *J Mol Struct*, 2013, **1048**, 267-273.
28. H. Zhang, C. Guo, X. Wang, J. Xu, X. He, Y. Liu, X. Liu, H. Huang and J. Sun, *Cryst. Growth Des.*, 2013, **13**, 679-687.
29. H. Lin, S.-G. Zhu, L. Zhang, X.-H. Peng and H.-Z. Li, *J. Energ. Mater.*, 2013, **31**, 261-272.
30. B. Gao, D. Wang, J. Zhang, Y. Hu, J. Shen, J. Wang, B. Huang, Z. Qiao, H. Huang, F. Nie and G. Yang, *J. Mater. Chem. A*, 2014, **2**, 19969-19974.
31. D. Spitzer, B. Risse, F. Schnell, V. Pichot, M. Klaumunzer and M. R. Schaefer, *Sci Rep-Uk*, 2014, **4**.
32. Y. P. Wang, Z. W. Yang, H. Z. Li, X. Q. Zhou, Q. Zhang, J. H. Wang and Y. C. Liu, *Propellants, Explos., Pyrotech.*, 2014, **39**, 590-596.
33. H. Lin, S.-G. Zhu, H.-Z. Li and X.-H. Peng, *J Phys Org Chem*, 2013, **26**, 898-907.
34. Z. Yang, H. Li, H. Huang, X. Zhou, J. Li and F. Nie, *Propellants, Explos., Pyrotech.*, 2013, **38**, 495-501.
35. C. Zhang, Y. Cao, H. Li, Y. Zhou, J. Zhou, T. Gao, H. Zhang, Z. Yang and G. Jiang, *CrystEngComm*, 2013, **15**, 4003-4014.
36. A. D. Bond, *CrystEngComm*, 2007, **9**, 833-834.
37. F. Lara-Ochoa and G. Espinosa-Pérez, *Supramol Chem*, 2007, **19**, 553-557.
38. A. T. Nielsen, R. A. Nissan, D. J. Vanderah, C. L. Coon, R. D. Gilardi, C. F. George and J. Flippen-Anderson, *J Org Chem*, 1990, **55**, 1459-1466.
39. C. Zhang, X. Xue, Y. Cao, J. Zhou, A. Zhang, H. Li, Y. Zhou, R. Xu and T. Gao, *CrystEngComm*, 2014, **16**, 5905-5916.
40. R. Simpson, P. Urtiew, D. Ornellas, G. Moody, K. Scribner and D. Hoffman, *Propellants, Explos., Pyrotech.*, 1997, **22**, 249-255.
41. D. I. A. Millar, H. E. Maynard-Casely, D. R. Allan, A. S. Cumming, A. R. Lennie, A. J. Mackay, I. D. H. Oswald, C. C. Tang and C. R. Pulham, *CrystEngComm*, 2012, **14**, 3742-3749.
42. U. Nair, R. Sivabalan, G. Gore, M. Geetha, S. Asthana and H. Singh, *Combustion, Explosion and Shock Waves*, 2005, **41**, 121-132.
43. V. M. Boddu, D. S. Viswanath, T. K. Ghosh and R. Damavarapu, *J Hazard Mater*, 2010, **181**, 1-8.
44. A. K. Nandi, N. Thirupathi, A. K. Mandal and R. K. Pandey, *Cent. Eur. J. Energ. Mater.*, 2014, **11**, 295-305.
45. B. M. Dobratz, *Properties of chemical explosives and explosive simulants*, comp. and ed.; California Univ., Livermore (USA). Lawrence Livermore Lab., 1972.
46. J. R. Kolb and H. Rizzo, *Propellants, Explos., Pyrotech.*, 1979, **4**, 10-16.
47. C. Zhang, X. Wang and H. Huang, *J Am Chem Soc*, 2008, **130**, 8359-8365.
48. W. Selig, *Estimation of the Solubility of 1, 3, 5-triamino-2, 4, 6-trinitrobenzene (TATB) in Various Solvents*, California Univ., Livermore (USA). Lawrence Livermore Lab., 1977.
49. A. E. van der Heijden and R. H. Bouma, *Cryst. Growth Des.*, 2004, **4**, 999-1007.
50. M. A. Elbagerma, H. G. M. Edwards, T. Munshi, M. D. Hargreaves, P. Matousek and I. J. Scowen, *Cryst. Growth Des.*, 2010, **10**, 2360-2371.
51. H. G. Brittain, *Cryst. Growth Des.*, 2009, **9**, 2492-2499.
52. H. G. Brittain, *Cryst. Growth Des.*, 2009, **9**, 3497-3503.
53. H. G. Brittain, *Cryst. Growth Des.*, 2010, **10**, 1990-2003.
54. M. Ghosh, V. Venkatesan, N. Sikder and A. K. Sikder, *Cent. Eur. J. Energ. Mater.*, 2013, **10**.
55. M. Ghosh, V. Venkatesan, S. Mandave, S. Banerjee, N. Sikder, A. K. Sikder and B. Bhattacharya, *Cryst. Growth Des.*, 2014, **14**, 5053-5063.
56. R. Turcotte, M. Vachon, Q. S. M. Kwok, R. Wang and D. E. G. Jones, *Thermochim Acta*, 2005, **433**, 105-115.
57. H. Muthurajan, R. Sivabalan, M. B. Talawar and S. N. Asthana, *J Hazard Mater*, 2004, **112**, 17-33.
58. L. Rothstein and R. Petersen, *Propellants, Explos., Pyrotech.*, 1979, **4**, 56-60.
59. L. R. Rothstein, *Propellants, Explos., Pyrotech.*, 1981, **6**, 91-93.